

Conductive ZnO-ZnGaON nanowire-array-on-a-film photoanode for stable and efficient sunlight water splitting

Electronic Supplementary Information

Miao Zhong,^a Yanhang Ma,^b Peter Oleynikov,^b Kazunari Domen^a and Jean-Jacques Delaunay^{*a}

^a School of Engineering, The University of Tokyo, 7-3-1 Hongo, Bunkyo-Ku, Tokyo 113-8656 (Japan). E-mail: jean@mech.t.u-tokyo.ac.jp; Fax: +81-3-5841-0441; Tel: +81-3-5841-3017

^b Department of Materials and Environmental Chemistry, Stockholm University, SE-10691 Stockholm, Sweden.

1. Effect of the growth temperature on the quality of ZnO-ZnGaON nanowires

We study the effect of the second CVD process temperature on the quality of the ZnO-ZnGaON nanowires. As shown in the table in Figure S1, the ZnO-ZnGaON nanowire samples were synthesized at different ZnO nanowire-array-on-a-film substrate temperature with a constant ammonia flow rate of 30 sccm for 20 minutes. It is found that the nanowire morphologies were mainly maintained after the second CVD process when the substrate temperatures was lower than 900 °C (see SEM images in Figure S1). With higher substrate temperatures above 900 °C, ZnO nanowires were totally etched by ammonia gas.

As shown in the diffuse reflectance spectra in Figure S1, the light absorption edges of the synthesized ZnO-ZnGaON nanowire samples shifted to longer wavelength with the increase in the substrate temperature, indicating more Ga and N were incorporated into the ZnO nanowires. However, the resistance of the synthesized ZnO-ZnGaON nanowire samples also increased with the increase in the substrate temperature. This is likely because N incorporation became difficult to control at a temperature above 850 °C, when using corrosive NH₃ gas as a precursor in the CVD process. It is inferred that a large number of ruinous defects was formed in the ZnO nanowires. As a result, the ZnO-ZnGaON-3 sample had an estimated sheet resistance over MΩ/□ and the ZnO-ZnGaON-4 nanowire sample was non-conductive. In contrast, the sheet resistances of the ZnO-ZnGaON-1 and ZnO-ZnGaON-2 samples were below 100 Ω/□ and the sheet resistance of the ZnO-ZnGa₂O₄ sample was below 10 Ω/□. Thus, there is a balance between the increase in light absorption and conductivity for improved PEC water splitting performance.

Synthesis conditions in the second CVD process for the nanowire samples (b-f)

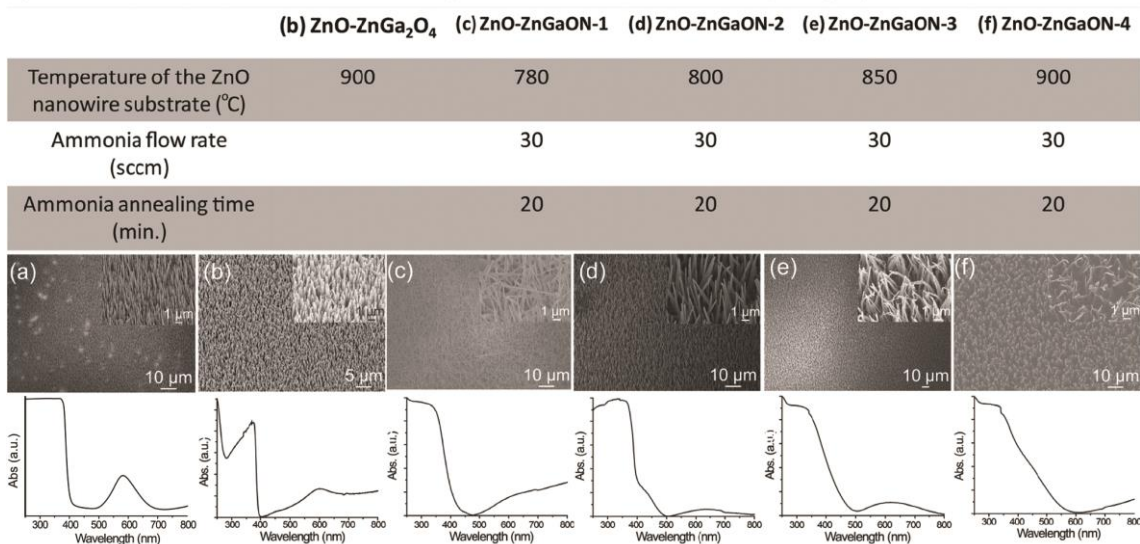


Figure S1 Growth conditions, SEM images, and UV-VIS diffuse reflectance spectra of the ZnO, ZnO-ZnGa₂O₄ and ZnO-ZnGaON nanowire samples.

2. XPS analyses of the ZnO and ZnO-ZnGaON nanowire array on a film samples

Figure S2 presents the enlarged XPS results of the ZnO and ZnO-ZnGaON nanowire array on a film samples. The detailed discussions are presented in the manuscript.

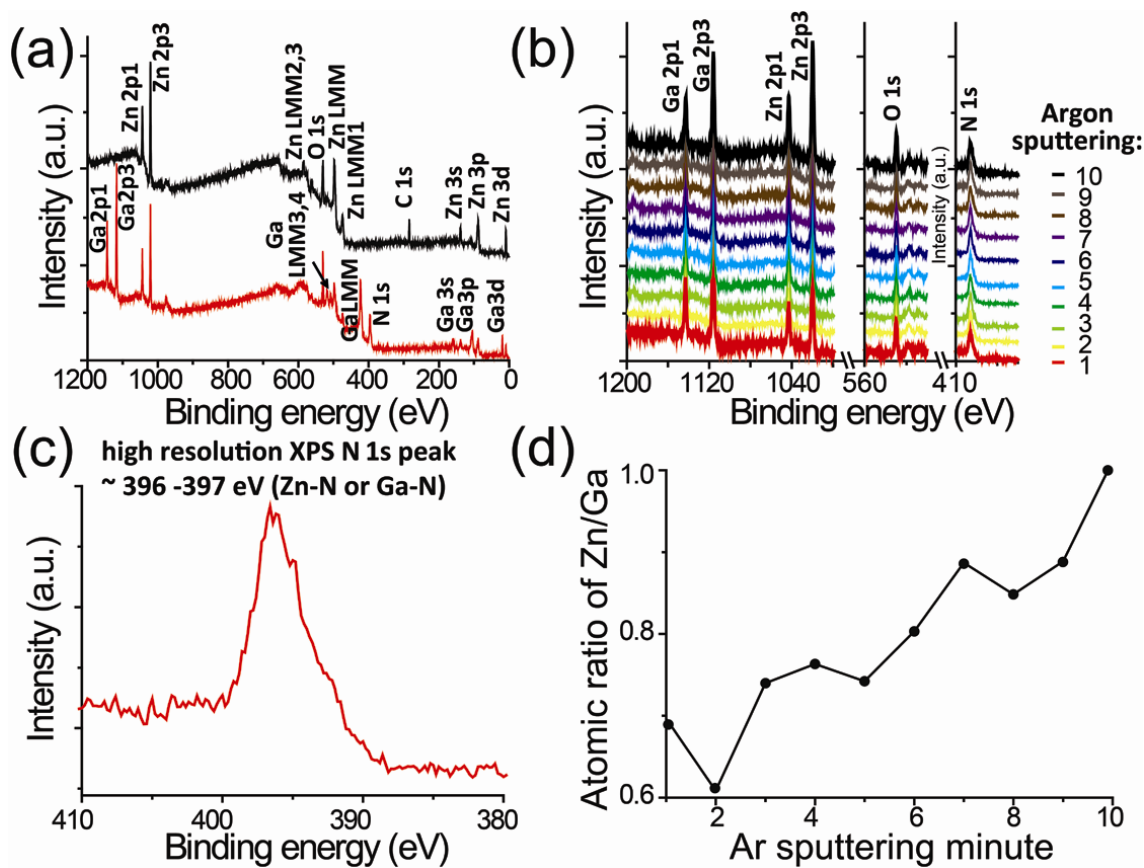


Figure S2 XPS analyses of the ZnO and ZnO-ZnGaON nanowire-array-on-a-film samples: (a) wide-scan XPS survey spectra of the ZnO and ZnO-ZnGaON samples; (b) XPS depth profile spectra of the ZnO-ZnGaON sample; (c) high resolution XPS spectrum of the N 1s peak in the ZnO-ZnGaON samples; (d) estimated Zn/Ga atomic ratio in the ZnO-ZnGaON sample from the XPS depth profile analysis.

3. XRD analyses for the ZnO and ZnO-ZnGaON nanowire array on a film samples

Figure S3 presents the enlarged XRD pattern and SEM images of the ZnO and ZnO-ZnGaON nanowire array on a film samples with different nanowire length and film thickness.

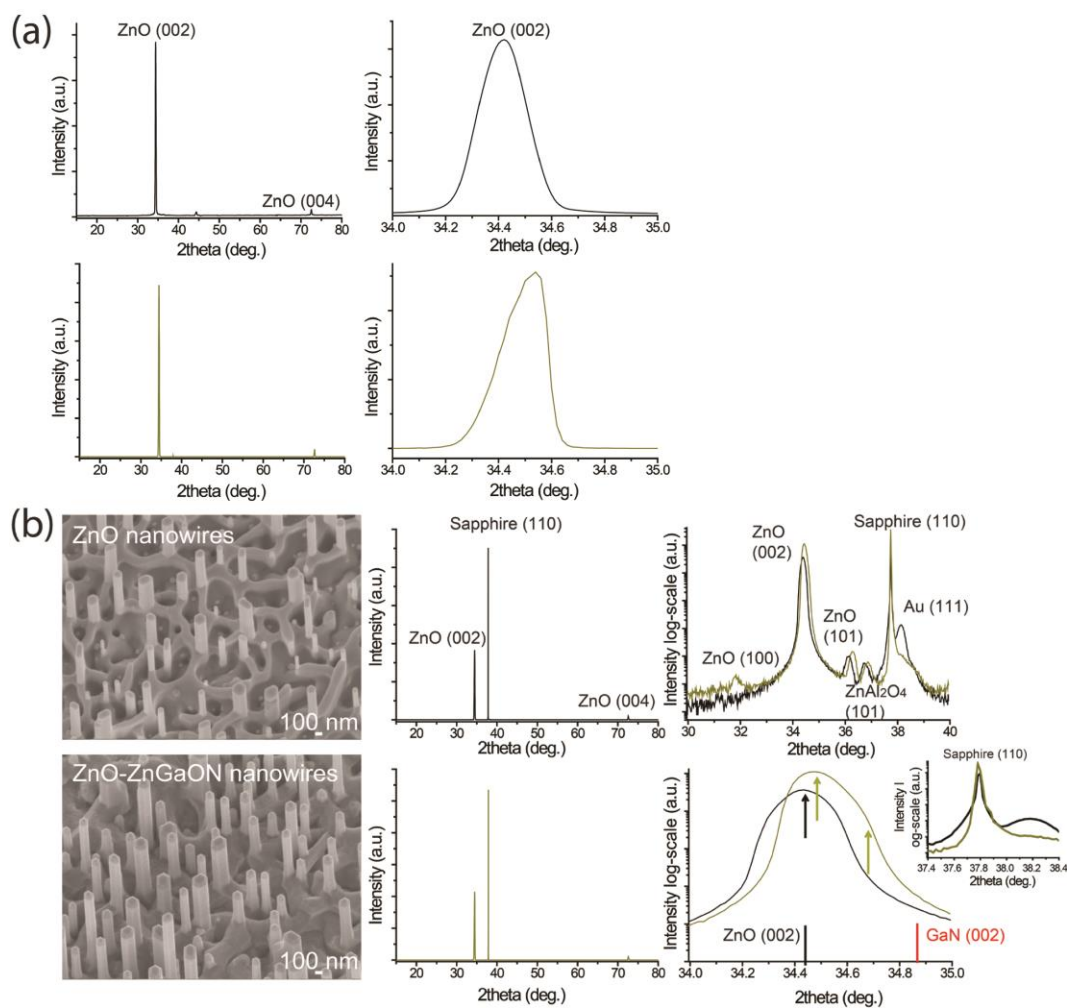


Figure S3 XRD θ - 2θ measurements of the synthesized ZnO and ZnO-ZnGaON nanowire-array-on-a-film photoanodes. (b) SEM images (left) and XRD θ - 2θ measurements (right) of the ZnO and ZnO-ZnGaON short nanowire on thin film samples.

4. Electro-impedance spectroscopy (EIS) and photoelectrochemical (PEC) current-potentiometry scan of the ZnO and ZnO-ZnGaON nanowire-array-on-a-film samples

Figure S4 presents the EIS and current-potentiometry data of the ZnO, ZnO-ZnGa₂O₄, ZnO-ZnGaON-1 and ZnO-ZnGaON-2 photoanodes. The EIS analyses of the photoanodes were performed using a three-electrode electrochemical configuration in a 0.5 M Na₂SO₄ solution at pH = 7 under dark condition. The light on-off current-potentiometry scan was performed using a three-electrode electrochemical configuration in a non-sacrificial electrolyte of 0.5 M Na₂SO₄ solution buffered with NaOH at pH = 13 under sunlight and 300 W Xenon lamp illumination respectively. All the EIS curves of $(1/C_S)^2$ versus voltage showed positive slopes, indicating n-type characteristic of the ZnO, ZnO-ZnGa₂O₄ and ZnO-ZnGaON nanowires. The estimated carrier density of the ZnO, ZnO-ZnGa₂O₄ and ZnO-ZnGaON-1 and ZnO-ZnGaON-2 were $\sim 10^{17} \text{ cm}^{-3}$, $\sim 5 \times 10^{20} \text{ cm}^{-3}$, $\sim 10^{18} \text{ cm}^{-3}$ and $\sim 5 \times 10^{18} \text{ cm}^{-3}$ respectively. It is therefore inferred that Ga was a strong donor to ZnO and a controlled incorporation of Ga into ZnO could increase the electron concentration in the nanowires. The PEC current-potentiometry results of the ZnO, ZnO-ZnGa₂O₄, ZnO-ZnGaON-1 and ZnO-ZnGaON-2 photoanodes were measured under sunlight and 300 W Xenon lamp illumination. It is revealed that the ZnO-ZnGaON-2 photoanode had the best photo-oxidation performance because of the conductive and visible-light-sensitive nanowire-array-on-a-film structure. The photocurrent density of the ZnO-ZnGaON-2 photoanode was $\sim 1.7 \text{ mA/cm}^2$ under sunlight illumination and $\sim 16 \text{ mA/cm}^2$ under 300 W Xenon lamp illumination at an applied voltage of $1.2 V_{RHE}$. It is also found that the ZnO and ZnO-ZnGaON-1 photoanodes had similar PEC performance of $\sim 1.2 \text{ mA/cm}^2$ under sunlight illumination and $\sim 9\text{-}10 \text{ mA/cm}^2$ under 300 W Xenon lamp illumination at an applied voltage of $1.2 V_{RHE}$. Importantly, the ZnO-ZnGaON-1 photoanode also had a strong anti-photocorrosive ability, which was similar to the ZnO-ZnGaON-2 photoanode. SEM observations of the ZnO-ZnGaON-1 sample showed no noticeable degradation of the nanowire structure before and after 6 hours of PEC amperometric test. This is evidence for the stabilization of the ZnO nanowires with the formation of ZnGaON material. Finally, the ZnO-ZnGa₂O₄ photoanode had the lowest photocurrent density under sunlight and 300 W Xenon lamp illumination. The formation of wide band gap ($\sim 4 \text{ eV}$) ZnGa₂O₄ on the surface of the nanowires prevents the absorption in the 3.1-4 eV range of UV light to some extent and, thus, lower the water photooxidation current. In addition, the largely increased electron density in the ZnO-ZnGa₂O₄ nanowires also decreased the hole lifetime in the nanowires and thus the photooxidation performance is reduced.

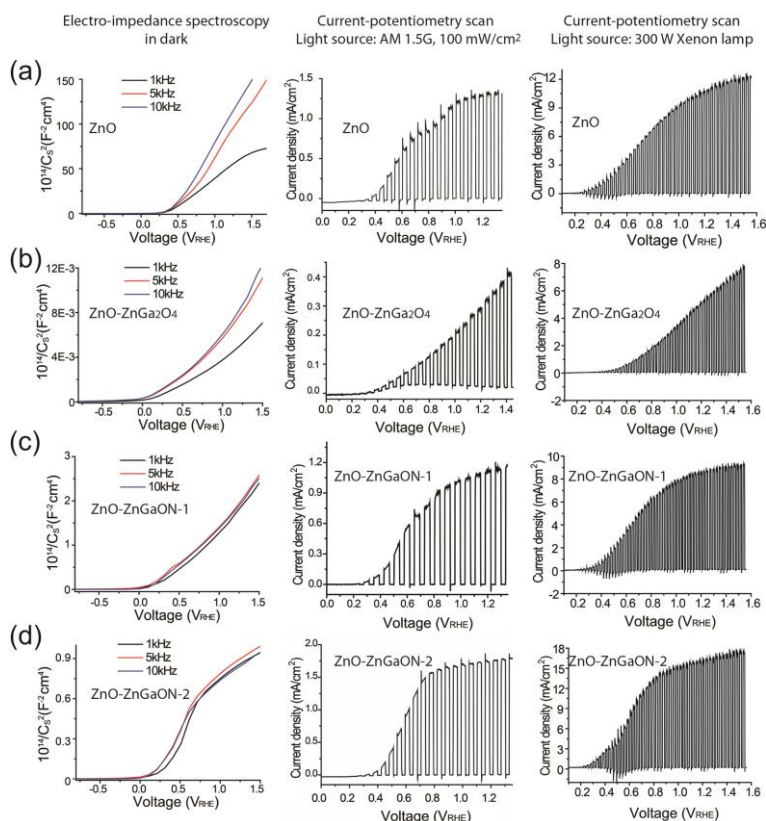
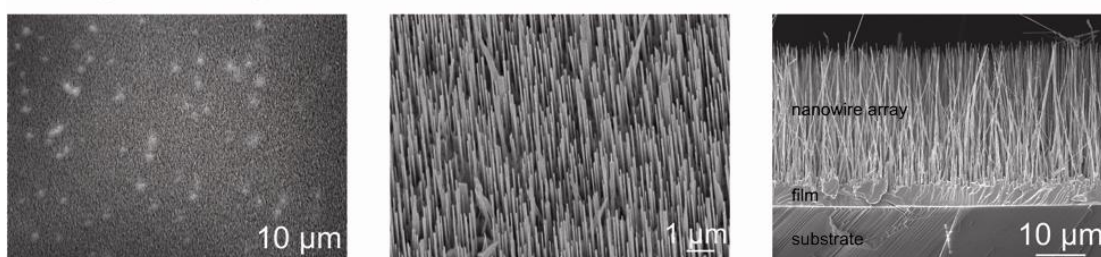


Figure S4 EIS and current-potentiometry curves of the ZnO, ZnO-ZnGa₂O₄ and ZnO-ZnGaON nanowire photoanodes.

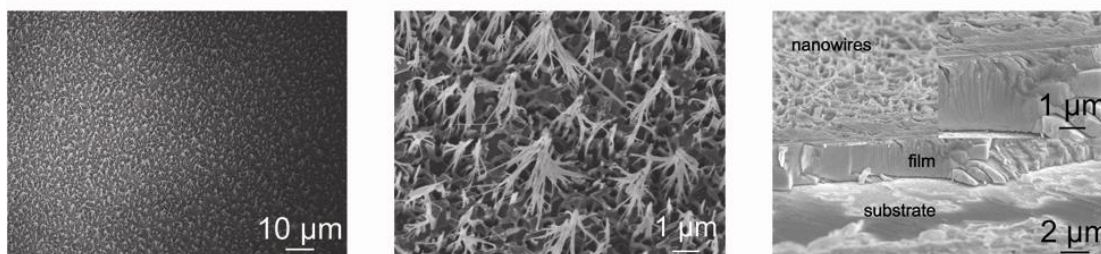
5. In-time observation of the morphology change of the ZnO nanowire-array on a film photoanode during PEC amperometric test

Figure S5 shows the top and cross-sectional SEM images of the ZnO nanowire array on a film photoanode for different PEC stability measurement times. It is clearly seen that the morphology of the ZnO photoanode is changed from nanowire array on a film to nanoporous film after 5.5-hour PEC stability test. The thickness of the bottom ZnO film also decreased to $\sim 2\ \mu\text{m}$ from its original value of over $5\ \mu\text{m}$. Finally, the ZnO nanoporous film was totally etched out after soaking the sample in the same electrolyte of $0.5\ \text{M}\ \text{Na}_2\text{SO}_4$ pH 13 for another 9 hours under dark condition. The photocurrent of the etched photoanode decreased to $\sim 30\ \mu\text{A}/\text{cm}^2$ at $1.2\ \text{V}_{\text{RHE}}$ from the original $1.5\ \text{mA}/\text{cm}^2$ at $1.2\ \text{V}_{\text{RHE}}$. It is therefore confirmed that the ZnO photoanode was chemically instable in alkaline solution. In the case of our ZnO-ZnGaON nanowire-array-on-a-film photoanode, the estimated diameter of the nanowires did not change before and after 5.6 hours PEC stability test in $0.5\ \text{M}\ \text{Na}_2\text{SO}_4$ pH 13 solution, indicating a strong anticorrosive ability of the ZnGaON surface.

SEM image of the ZnO photoanode before PEC measurement



SEM image of the ZnO photoanode after 1 hour PEC measurement



SEM image of the ZnO photoanode after 5.5 hours PEC measurement

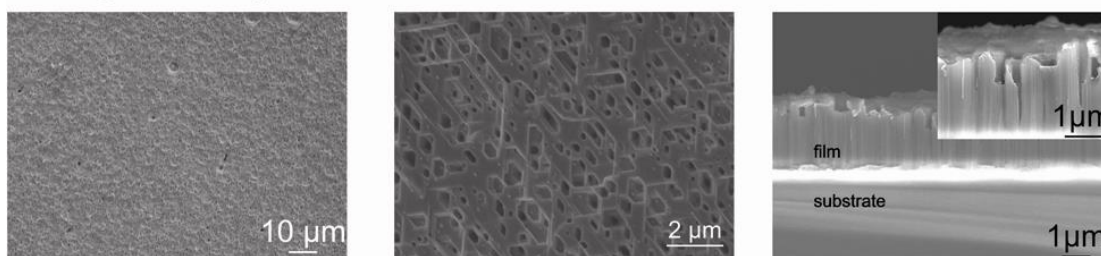


Figure S5 SEM images of the ZnO nanowire array on a film photoanode before and after PEC amperometric test.